On the quality of unsupported overhangs produced by laser powder bed fusion

On the quality of unsupported overhangs produced by laser powder bed fusion

Gabriele Piscopo*, Alessandro Salmi and Eleonora Atzeni

Politecnico di Torino,
Department of Management and Production Engineering (DIGEP),
Corso Duca degli Abruzzi, 24, 10129, Torino, Italy
Email: gabriele.piscopo@polito.it
*Corresponding author

Abstract: One of the main design constraints for additive manufacturing is the definition of downward-facing surfaces, which can lead to problems, like part failing or warping, during construction and poor surface quality. In this paper, a specific index has been defined to represent the surface quality of the downward-facing surfaces induced by the laser powder bed fusion (L-PBF) process. In order to validate the quality index, a design of experiment (DoE) that considers geometric parameters of the overhangs has been defined and carried out, and the quality of resulting surfaces has been evaluated using an optical scanning system. The statistical analysis (ANOVA) has allowed identifying the relationships between significant geometrical parameters and the quality index here proposed.

[Submitted 5 April 2018; Accepted 27 August 2018]

Keywords: additive manufacturing; selective laser melting; SLM; powder bed fusion; PBF; unsupported overhangs; surface quality; process parameters; roughness; optical scanning system.

Reference to this paper should be made as follows: Piscopo, G., Salmi, A. and Atzeni, E. (2019) 'On the quality of unsupported overhangs produced by laser powder bed fusion', *Int. J. Manufacturing Research*, Vol. 14, No. 2, pp.198–216.

Biographical notes: Gabriele Piscopo received his BS and MS degrees in Mechanical Engineering from the Politecnico di Torino, Italy, in 2016. From 2016, he was a PhD student and Research Fellow with the Department of Management and Production Engineering, Politecnico di Torino. His research interests include additive manufacturing (AM), FEM process simulation and structural optimization.

Alessandro Salmi received his PhD degree in Production Engineering from Politecnico di Torino in 2008 after graduating in Mechanical Engineering. He is an Associate Professor of Manufacturing Technology and Systems at Politecnico di Torino. He is the author and/or co-author of one book and more than 45 publications. His research interests include AM process and design optimization, high speed machining (HSM), and FE process simulation. He was one of the authors who won the Best Young Scientist Award at the *4th International Conference on Additive Technologies (iCAT)* in 2012.

Eleonora Atzeni received her PhD degree in Industrial Production System Engineering from Politecnico di Torino in 2005 after graduating in Mechanical Engineering. She is an Associate Professor of Manufacturing Technology and Systems at Politecnico di Torino. She is the author of more than 65 publications. Her research interests include AM post-processing and FE process simulation, high speed machining (HSM), and joining. Her awards include the Best Young Scientist Award at the *4th International Conference on Additive Technologies (iCAT)* in 2012 and the Best Paper Award at the *International Conference on Innovative Design and Manufacturing (ICIDM)* in 2014.

1 Introduction

Additive manufacturing (AM) is defined by ASTM standard as the "process of joining materials to make parts from 3D model data, usually layer upon layer, as opposed to subtractive manufacturing and formative manufacturing methodologies" (ISO/ASTM52900-15, 2015). By AM, parts with complex geometries are directly produced from computer-aided design (CAD) models of the components, without the use of tools or equipment, as jig or complex hold systems. The first application of AM dates back to 1980s, named rapid prototyping (RP), to shorten the time for the fabrication of prototypes. Then, the technological development allowed the use of AM as a tool for producing final parts, even of metals (Gu, 2015). The main industrial applications of the AM processes are in the biomedical, aerospace and automotive sectors, whose products are characterised by a high level of personalisation, complexity and a relatively small production volume. For these sectors, the use of AM allows to obtain economic benefits. This was proved by Atzeni et al. (2010a), that in 2010 demonstrated that AM of plastic parts is economically convenient for medium lot production, later, in 2012, Atzeni and Salmi performed a cost analysis and established that AM is also adequate for small to medium batch sizes of end-usable metal parts.

Today, the increasing knowledge of the relationships between process parameters and the characteristics of the produced part allows the extensive use of AM processes for the production of final parts in different application fields. For instance, Jardini et al. (2014) showed that the use of laser powder bed fusion (L-PBF) could provide benefits in surgery procedures regarding the duration of the operation and also in the surgical accuracy. In their work, AM is used for the realisation of biomodel and customised implant during the reconstruction of large cranial defects. Baudana et al. (2016) showed the feasibility of electron beam melting (EBM) in the production of automotive turbocharger wheels. They also showed that using EBM it is possible to modify the design of the turbocharger in order to reduce the component weight. Nevertheless, one of the most promising field in which AM could produce the main benefits, due to the lightweight potentialities, is the aeronautical sector (Herzog et al., 2016). Liu et al. (2017) performed an extensive analysis on the application of AM in aerospace applications. In their work, authors summarised the characteristics of components favouring AM production and explained the benefits of using AM for creating aerospace components, analysing three different applications: production of metal components by directed energy deposition (DED) or powder bed fusion (PBF) processes, production of non-metallic components by fused

deposition modelling (FDM) and repair applications. Focusing the attention on metal parts production, L-PBF, also known as selective laser melting (SLM) or direct metal laser sintering (DMLS), is one of the most powerful AM process. Developed and commercialised by EOS GmbH in Germany (Gao et al., 2015; Shellabear and Nyrhilä, 2004), L-PBF uses a focused laser beam to melt a thin layer of a pre-spread bed of metal powder in order to create the section of the part according to the STL model and the slicing data. Repeating the process it is possible to produce fully dense metal parts with complex geometries and with mechanical properties comparable with the properties of bulk material (Gu et al., 2012).

Although it is possible to produce parts with complex shapes, it should be noted that they generally require support structures to be built. Support structures anchor the parts to the building platform and allow to reduce distortions (Brackett et al., 2011). They constitute a thermal exchange surface and consequently, the heat of the melt pool is dissipated and the residual stresses and the distortions are lower (Gan and Wong, 2016). However, support structures represent a waste in term of material and require time for their construction and removal. Thus, in the AM production practice, supports are minimised and self-supporting (or unsupported) surfaces are preferred by a proper design and orientation of the part. From the literature, it is possible to observe that only few researches investigated the effect of geometrical parameters on the quality of unsupported surfaces. Most of them are focused on the evaluation of the quality obtainable on steel components. Fox et al. (2016) established that process parameters and overhang angle have a great influence on surface roughness by means of a qualitative and a quantitative analysis on stainless steel samples, but they did not found a clear correlation between the roughness and the process parameters. Wang et al. (2013b) investigated the effects of surface angle, scanning speed, laser power, stress accumulation and scanning vector length on the quality of AISI 316L overhang surfaces; they indicated two different methods in order to improve the surface quality: by adjusting the orientation of the part and by controlling local energy input. Thomas (2009) performed an extensive analysis on the influence of geometrical parameters on the accuracy of AISI 316L unsupported surfaces. In his work, the author demonstrated that overhangs with an inclination greater than 45º required support structure to avoid part failure. In addition, he showed that the surface roughness of the overhangs decreases if the value of surface inclination decreases. His work also showed that is not possible to produce fillets with tangential radius without the use of support structure and consequently, he proposed different geometries varying the inclination angle of the fillets. Strano et al. (2013) performed an experimental analysis on the surface roughness on AISI 316L parts and they observed that the value of the roughness was influenced by the inclination angle of the surface. They proposed a mathematical model, which includes the effect of the presence of particle on the surface, for predicting the surface roughness. Other papers analyse the quality achievable on aluminium alloy parts. Calignano et al. (2013) used a fractional factorial design of experiment (DoE) in order to determine the significance of process parameters on the surface roughness of AlSi10Mg parts and, as a result, they found that scan speed has the greatest influence. Atzeni and Salmi (2015) performed a DoE in order to evaluate the significant factors on the dimensional tolerances of self-supporting faces on AlSi10Mg samples; the result of their statistical analysis indicated that the angle of inclination, the overhangs ledge and the curvature of the surface strongly influence the dimensional tolerance of the components. Moreover, an interaction was observed between curvature and angle of inclination. This literature review provides some

important considerations on the L-PBF process and the resulting part quality. First, the control of process parameters is of great importance, since they directly affect the surface quality. Secondly, geometrical parameters of overhangs highly influence the quality of the surface, but the inherent variability of the process does not allow to find a clear model describing the effect of geometrical variables and their correlations. Thus, only statistical tools could be used to predict in which way geometrical parameters can affect the quality of the resulting surface.

In this paper, the influence of geometrical parameters on the surface quality of AlSi10Mg unsupported features is analysed using a statistical approach. To this aim, a specific quality index is defined, combining the geometrical mean deviation and the range of its variation. The proposed quality index is used as response variable of a 4^3 full factorial DoE plan. Accordingly, a set of overhanging surfaces, produced by means of a L-PBF machine, are measured through an optical three-dimensional measuring system. The significance of geometrical factor as the curvature of the surface, surface angle and the extension of overhang are investigated. The result is a statistical model able to predict the achievable surface quality of AlSi10Mg parts.

2 Overhangs: geometrical parameters

In the literature, several rules relating to the overhang design are defined. For example, it is well known that it is not possible to produce an overhang parallel to the building platform without the use of support structures if the overhang exceeds 1.5 mm length for AISI 316L (Thomas, 2009) or 2 mm length for aluminium alloy (Vora et al., 2015). The need of support structures increases the build time and the cost per part therefore flat or curved self-supporting geometries are preferable.

Figure 1 Effect of the angle α on the surface roughness (see online version for colours)

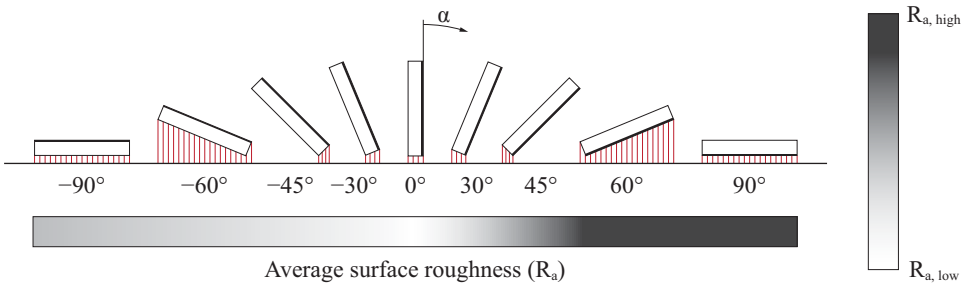

Concerning downward-facing flat surfaces, Wang et al. (2013a) showed that in case of AISI 316L an overhang surface with an inclination of less than 35º requires support to prevent warping effects; if the inclination is greater than 40º, instead, the overhang is well produced. Thomas (2009), considering 20 × 20 × 5 mm^3 sample parts of AISI 316L, found equivalent results and demonstrated that for unsupported overhangs the downward-facing surface roughness increases if the inclination increases (Figure 1). Calignano (2014) studied the geometrical limits of self-supporting surfaces for AlSi10Mg and Ti6Al4V components. The author found that it is possible to fabricate inclined surfaces without supports up to 30º, but in the case of AlSi10Mg the surface quality was

poorer. Besides regarding downward-facing curve surfaces, Thomas (2009) found that it is possible to produce concave fillets with radii up to 3 mm and convex fillets up to 2 mm without support structures; however, the accuracy of these surfaces was poor. To improve surface quality, or to extend the overhang length, alternative radii design could be considered, for example by varying the tangent at the starting and ending points. These rules are defined for AISI 316L parts. Calignano (2014), analysing overhangs with fillets on AlSi10Mg parts, determined that for concave radii the upper point is the most critical one and the quality can be improved if the tangent angle increases. On the contrary, for convex radii, the lower point of the curved surface is the most critical one.

Following these outcomes and according to Atzeni and Salmi (2015), an overhang feature, can be defined by considering basically three geometrical parameters that are shown in Figure 2(a): the angle α of the surface (in case of curved surfaces is the angle of the line between A and B) with respect to the building platform, the radius R of curved surfaces and the length Δx of the overhang.

3 Definition of the surface quality index *k*

The surface quality could be evaluated by measuring the surface roughness and by measuring the deviations of the surface from the ideal geometry (geometrical tolerance). In this paper the focus is on geometrical quality, since errors in the geometry could make the component useless. For the inspection of complex geometries, such those typical of the AM production, optical systems are very powerful and are preferred to classical coordinate measuring machines (CMMs) as demonstrated in the literature (Iuliano and Minetola, 2009; Iuliano et al., 2010; Minetola, 2012; Minetola et al., 2012). The reason is that contactless systems provide faster scan time and a high quantity of measured points than CMMs. The accuracy of an optical scanner depends on the working area and on the working distance. Calibrating the scanner on a working area of 160 × 200 mm^2 and a working distance of 600 mm the accuracy is 0.06 mm as declared in the device datasheet. Moreover, the repeatability of the used scanner was proved by Minetola et al. (2012). Consequently, optical scanners with a resolution up to 0.06 mm allow measurement of the deviation with an adequate accuracy, being the L-PBF tolerance of around 0.1 mm (Atzeni et al., 2010b, 2013; Salmi et al., 2014).

The data resulting from the scanning operation are compared with nominal data to retrieve information about the geometrical errors induced by the manufacturing process. To perform the statistical analysis, in this paper a surface quality index k is defined that combines information about the mean deviation of the actual surface from the nominal one, and the range of the variation. In detail, the surface quality index k is defined as

$$k = (1 + m^2) \cdot r \tag{1}$$

where m is the mean deviation of the surface and r is the range of variation defined as the difference between the maximum and the minimum value of the deviation of the overhang surface. The mean deviation provides an indication about the relevance of the deviation; the difference between the maximum and the minimum value of deviation, instead, provides information regarding the variability of data. The surface quality index k gives a combination of the two effects and qualitatively provides a comprehensive view of the surface quality of the overhang surface. Especially, the surface quality index k

tends to zero as m and r tend. If the mean deviation is zero, that is positive and negative contributions are equals, the surface quality index k is defined by the range of variation. If the range of variation is zero, the actual surface is identical to the nominal surface and the surface quality index k is zero. In general, the quality of the surface increases as the quality index k value decreases.

4 Materials and method

In industry, DoE is used to evaluate the effect of input variables, called factors, on the variation of the analysed output of the process, called response and to evaluate if there are some interactions between the analysed factors. Using DoE it is possible to reduce the time and the cost required to optimise the product and the process (Tanco et al., 2007). The proposed surface quality index k was used as response variable of a 4^3 DoE, considering the previous work of Atzeni and Salmi (2015). The factors of the DoE were the geometrical parameters of the overhang and their levels are listed in Table 1. The full factorial DoEs were defined using Minitab® 17 software. A total of 64 different experiments were required.

Table 1 Geometrical factors and relative levels used in DoE

Factors	*Levels*
Overhang length, Δx (mm)	4.5, 6, 7.5, 9
Angle, α (º)	35, 37.5, 42.5, 45
Curvature, $1/R$ (mm^{-1})	–0.05, 0, 0.05, 0.1

Table 2 Sets of process parameters for the core, the skin and the contour used for the fabrication of the specimens

Parameters	*Skin*	*Core*	*Contour*
Scan speed (mm/s)	900	800	900
Laser power (W)	120	195	80
Hatch distance (mm)	0.10	0.17	-
Layer thickness (μm)		30	
Laser spot diameter (μm)		10	

A commercial aluminium alloy, EOS aluminium AlSi10Mg, was used for the experiment. Powder particles have a spherical shape and the average size is about 21–27 μm. The diameters corresponding to 10% (d_{10}), 50% (d_{50}) and 90% (d_{90}) of the cumulative size distribution are 19.3 μm, 40.7 μm and 74.8 μm, respectively (Manfredi et al., 2013). The specimens were produced using an EOSINT M 270 Dual Mode system. The system uses a 200 W Ytterbium fibre laser to melt the powder in an inert Argon atmosphere. A standard scanning strategy was adopted, which uses three different sets of process parameters for the core, the skin and the contour, respectively, as reported in Table 2 (Calignano et al., 2013). To improve the usefulness of the experimentation and in order to remove the sources of external variation, a randomisation was performed. Thus, the order and position of specimens on the building platform was defined based on the obtained randomisation. All the specimens were produced in a single job in order to

exclude the influence of possible external factors and to have the same initial conditions. Moreover, specimens had an angle of 15º respect the recoater direction to avoid some possible deformations induced by the recoater pressure, as represented in Figure 2(b). After production, the standard heat treatment for stress relieving at 300ºC for two hours was accomplished, then the samples were removed from the building platform. Specimens were not subjected to a shot-peening process in order to evaluate the as-built condition of overhang surfaces resulting from the L-PBF process. In fact, the shot-peening process induces changes of the surfaces conditions (Xie et al., 2016).

Figure 2 (a) Geometrical parameters of the overhangs (b) Details of the randomisation and arrangement of the specimens on the building platform (see online version for colours)

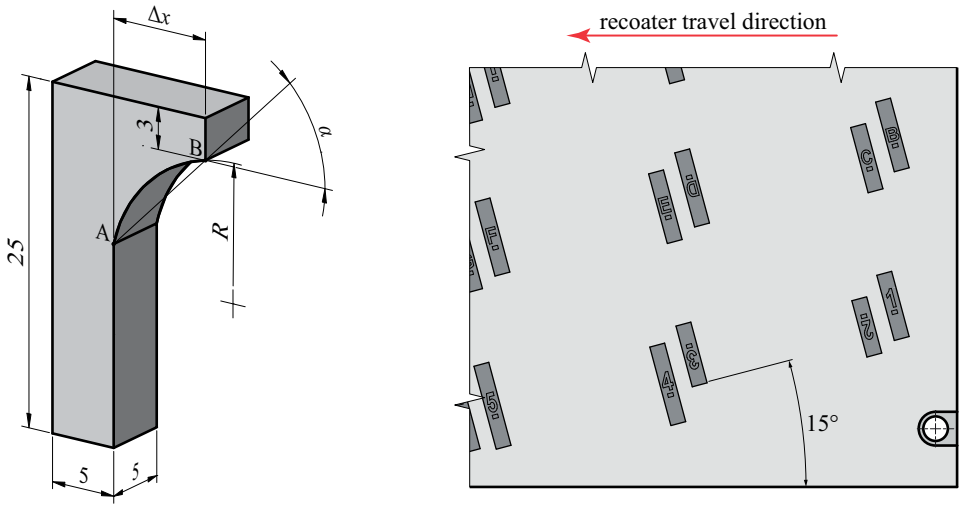

(a) (b)

Table 3 Technical specifications of ATOS standard

Specifications	*Values*
Sensor dimensions	610 × 160 × 125 mm^3
Sensor weight	2.5 kg
Scanning technique	Structured light
Scanning volume or area	From 100 × 80 × 80 mm^3 to 350 × 280 × 280 mm^3
Working distance	From 300 mm to 1100 mm
CCD camera resolution	768 × 572 pixels / 8 bits
Scanning time (per single view)	8 s
Accuracy	From 0.06 mm to 0.50 mm
Multiple scans registration	Automatic (by marker network)

The downward-facing surface of each specimen was measured using the structured light scanner ATOS standard produced by GOM GmbH. The technical specifications of the selected scanning device are reported in Table 3. Specimens were sprayed with a thin layer of white powder in order to reduce the reflectivity of the aluminium surfaces and to help the scanner to capture the data. This kind of powder does not influence the measurement results because the powder size is lower than scanner accuracy (Iuliano and Minetola, 2009). To exclude the influence of edge effects, on each examined surface a restricted area was identified considering a three-dimensional inner contour offset of 0.5 mm from the edges as illustrated in Figure 4(a). Then the restricted area was subjected to the analysis of deviation. Scanning data were then elaborated using the software GOM Inspect 2018 in order to evaluate the deviation error of each overhang surface (Minetola et al., 2015). Each acquired point cloud, after the elimination of erroneous data, was aligned to the nominal CAD data for surface comparison. The alignment was performed firstly using the pre-alignment tool; secondly a more accurate alignment was conducted using a best-fit procedure. The outputs for each specimen are a colour-coded deviation plot and the deviation values, given in form of a diagram and as a table, with the indication of the main statistic values such as maximum distance (*MAX*), minimum distance (*MIN*), mean distance, distance standard deviation, area of valid distance (*AVD*), integrated absolute distance, and the integrated distance (*ID*) that describes the volumetric deviation of the surface. For each specimen, outputs of the analysis are elaborated in order to evaluate:

- the mean deviation of the surface $m = I_D/A_{VD}$ that is defined as the ratio between the integrated distance and the area of valid distance, which is in turn the area of the surface under comparison
- the difference $r = MAX - MIN$ that is a measure of variation of the deviation
- the surface quality index k that is calculated according to equation (1).

Afterwards analysis of variance (ANOVA) was applied to the DoE in order to evaluate if the variation of the surface quality index k, selected as the response, was explained by the overhang geometrical factors selected in this study and to evaluate which factors were statistically significant. Lastly, a regression analysis was performed in order to model the relationship among the surface quality index k and the overhang geometrical parameters. This model will be used to estimate in advance the surface quality of overhanging surfaces.

5 Results and discussion

The unsupported surfaces defined by the different combinations of geometrical factors used in the DoE have been successfully produced. However, it was possible to observe defects like warpage and dross formation in some downward-facing surfaces. In particular, these problems occurred when the angle α was small (35º) and the overall length Δx was large (7.5 mm and 9 mm), and were localised near the lowest edge of the downwardly-facing concave surface and near the highest edge of the downwardly-facing convex surface in agreement with Calignano (2014).

Figure 3 (a) ATOS standard by GOM GmBH (b) and (c) 3D scanning of a specimen during the projection of the structured light pattern (d) Merging of the different acquired views (e) Generation of the mesh from the points cloud and exporting (see online version for colours)

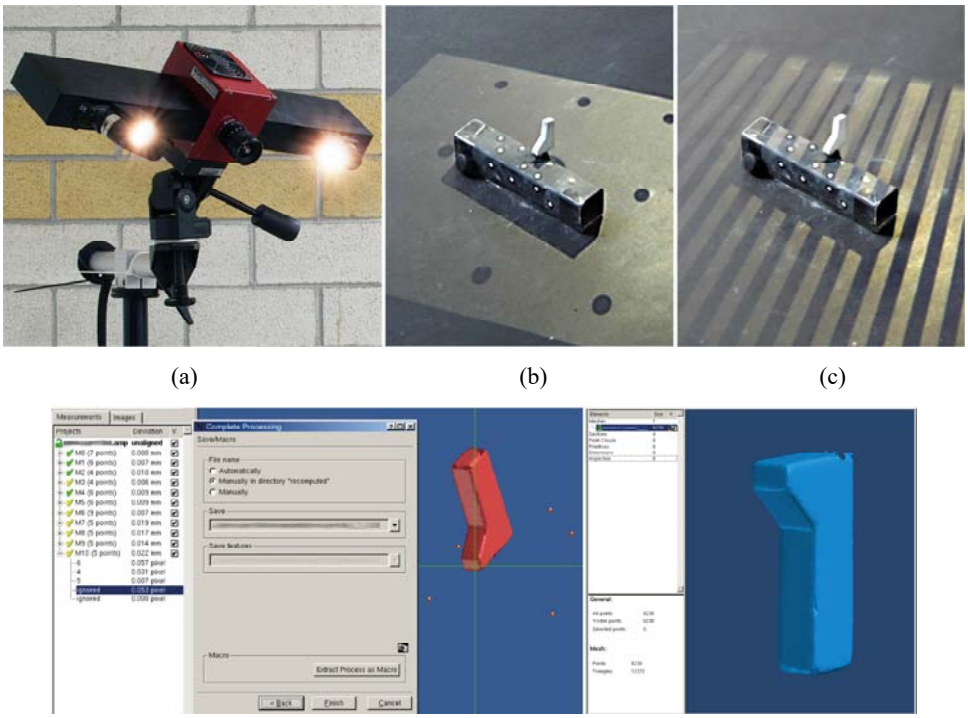

(a) (b) (c)

(d) (e)

Figure 4 (a) Example of a specimen, which corresponds to line 64, with visible edge effect on a concave surface and highlighted with red curves the contour of the restricted area used for the analysis of deviations (b) Results of the analysis performed using GOM inspect 2018 (see online version for colours)

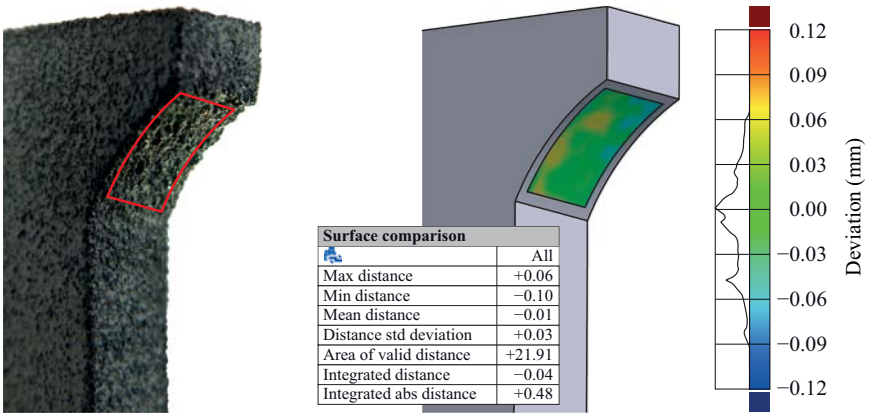

(a) (b)

Table 4 Results of the quality evaluation of downward-facing surfaces of the specimens

Line	Δx (*mm*)	$1/R$ (mm^{-1})	α (°)	*ID* (mm^2)	*AVD* (mm^2)	*m* (*mm*)	*MAX* (*mm*)	*MIN* (*mm*)	*R* (*mm*)	*k*
1	9	−0.05	35	−12.61	40.52	−0.31	−0.01	−0.57	0.56	0.61
2	9	−0.05	37.5	−11.66	42.01	−0.28	0.02	−0.48	0.50	0.54
3	9	−0.05	42.5	−2.79	45.62	−0.06	0.21	−0.18	0.39	0.39
4	9	−0.05	45	−1.85	47.81	−0.04	0.21	−0.17	0.38	0.38
5	9	0	35	1.52	39.95	0.04	0.09	−0.21	0.30	0.30
6	9	0	37.5	−0.53	41.38	−0.01	0.09	−0.15	0.24	0.24
7	9	0	42.5	−1.14	44.83	−0.03	0.10	−0.14	0.24	0.24
8	9	0	45	−5.58	46.91	−0.12	−0.03	−0.23	0.20	0.20
9	9	0.05	35	−10.69	40.52	−0.26	−0.07	−0.77	0.70	0.75
10	9	0.05	37.5	2.35	42.01	0.06	0.16	−0.18	0.34	0.34
11	9	0.05	42.5	1.60	45.62	0.04	0.12	−0.28	0.40	0.40
12	9	0.05	45	1.51	47.81	0.03	0.11	−0.11	0.22	0.22
13	*9*	*0.1*	*35*	*−3.22*	*42.52*	*−0.08*	*0.10*	*−0.89*	*0.99*	*1.00*
14	9	0.1	37.5	−3.53	44.25	−0.08	0.08	−0.70	0.78	0.78
15	*9*	*0.1*	*42.5*	*−6.17*	*48.52*	*−0.13*	*0.00*	*−0.96*	*0.96*	*0.98*
16	*9*	*0.1*	*45*	*−3.90*	*51.19*	*−0.08*	*0.10*	*−1.05*	*1.15*	*1.16*
17	7.5	−0.05	35	1.68	32.95	0.05	0.30	−0.09	0.39	0.39
18	7.5	−0.05	37.5	−0.49	34.18	−0.01	0.17	−0.18	0.35	0.35
19	7.5	−0.05	42.5	1.68	37.14	0.05	0.26	−0.08	0.34	0.34
20	7.5	−0.05	45	−3.19	38.94	−0.08	0.06	−0.20	0.26	0.26
21	7.5	0	35	−0.31	32.62	−0.01	0.12	−0.17	0.29	0.29
22	7.5	0	37.5	−1.82	33.81	−0.05	0.06	−0.18	0.24	0.24
23	7.5	0	42.5	2.53	36.69	0.07	0.20	0.03	0.17	0.17
24	7.5	0	45	−1.78	38.43	−0.05	0.06	−0.15	0.21	0.21
25	7.5	0.05	35	2.11	32.95	0.06	0.16	−0.24	0.40	0.40
26	7.5	0.05	37.5	0.70	34.14	0.02	0.15	−0.34	0.49	0.49
27	7.5	0.05	42.5	−0.46	37.14	−0.01	0.06	−0.22	0.28	0.28
28	7.5	0.05	45	−4.5	38.94	−0.12	−0.04	−0.25	0.21	0.21
29	*7.5*	*0.1*	*35*	*−4.43*	*34.04*	*−0.13*	*0.05*	*−0.87*	*0.92*	*0.94*
30	7.5	0.1	37.5	−1.00	35.44	−0.03	0.07	−0.54	0.61	0.61
31	7.5	0.1	42.5	−2.25	38.69	−0.06	0.05	−0.62	0.67	0.67
32	7.5	0.1	45	2.31	40.72	0.06	0.14	−0.46	0.60	0.60
33	6	−0.05	35	1.24	25.45	0.05	0.22	−0.26	0.48	0.48
34	6	−0.05	37.5	−1.07	26.43	−0.04	0.15	−0.20	0.35	0.35
35	6	−0.05	42.5	−5.53	28.78	−0.19	−0.04	−0.29	0.25	0.26
36	*6*	*−0.05*	*45*	*0.27*	*30.20*	*0.01*	*0.13*	*−8.57*	*8.70*	*8.70*
37	6	0	35	0.15	25.30	0.01	0.12	−0.18	0.30	0.30
38	6	0	37.5	−0.29	26.25	−0.01	0.09	−0.14	0.23	0.23
39	6	0	42.5	0.94	28.55	0.03	0.10	−0.08	0.18	0.18
40	6	0	45	0.79	29.94	0.03	0.10	−0.08	0.18	0.18

Table 4 Results of the quality evaluation of downward-facing surfaces of the specimens (continued)

Line	Δx (*mm*)	$1/R$ (mm^{-1})	α (°)	*ID* (mm^2)	*AVD* (mm^2)	*m* (*mm*)	*MAX* (*mm*)	*MIN* (*mm*)	*R* (*mm*)	*k*
41	6	0.05	35	3.43	25.46	0.13	0.21	−0.04	0.25	0.25
42	6	0.05	37.5	−0.99	26.43	−0.04	0.03	−0.20	0.23	0.23
43	6	0.05	42.5	1.14	28.78	0.04	0.13	−0.15	0.28	0.28
44	6	0.05	45	−1.21	30.20	−0.04	0.03	−0.18	0.21	0.21
45	6	0.1	35	1.90	26.00	0.07	0.19	−0.29	0.48	0.48
46	6	0.1	37.5	2.88	27.01	0.11	0.20	−0.21	0.41	0.41
47	6	0.1	42.5	2.88	29.52	0.10	0.17	−0.09	0.26	0.26
48	6	0.1	45	−0.69	31.05	−0.02	0.11	−0.19	0.30	0.30
49	4.5	−0.05	35	2.07	18.04	0.11	0.22	0.02	0.20	0.20
50	4.5	−0.05	37.5	1.58	18.72	0.08	0.21	−0.25	0.46	0.46
51	4.5	−0.05	42.5	1.47	20.51	0.07	0.16	−0.06	0.22	0.22
52	4.5	−0.05	45	0.54	21.56	0.03	0.14	−0.07	0.21	0.21
53	4.5	0	35	1.23	17.97	0.07	0.20	−0.08	0.28	0.28
54	4.5	0	37.5	1.15	18.69	0.06	0.25	−0.10	0.35	0.35
55	4.5	0	42.5	0.54	20.41	0.03	0.13	−0.12	0.25	0.25
56	4.5	0	45	0.77	21.46	0.04	0.13	−0.06	0.19	0.19
57	4.5	0.05	35	0.57	18.04	0.03	0.22	−0.21	0.43	0.43
58	4.5	0.05	37.5	0.95	18.77	0.05	0.12	−0.08	0.20	0.20
59	4.5	0.05	42.5	2.85	20.51	0.14	0.17	−0.07	0.24	0.24
60	4.5	0.05	45	2.14	21.56	0.10	0.14	−0.05	0.19	0.19
61	4.5	0.1	35	−2.37	18.26	−0.13	−0.06	−0.36	0.30	0.31
62	4.5	0.1	37.5	1.33	19.00	0.07	0.16	−0.15	0.31	0.31
63	4.5	0.1	42.5	2.82	20.81	0.14	0.25	−0.04	0.29	0.30
64	4.5	0.1	45	−0.04	21.91	0.00	0.06	−0.10	0.16	0.16

Figure 3 shows a specimen during the scanning operation and the elaboration of the points cloud. After three-dimensional scanning procedure, points clouds were elaborated and the results of the analyses are used to calculate the surface quality index *k*. Table 4 lists the surface quality index *k* obtained for the combinations of factors of the full factorial DoE. Figure 5 shows the distribution of the surface quality index *k* values calculated for the examined specimens. During the analysis of the results of the DoE, the presence of five outliers was identified, which could lead to errors during the analysis. The outliers are highlighted in Figure 5 and in the boxplot depicted in Figure 6. The outliers correspond to lines 13, 15, 16, 29 and 36 in Table 4. The outliers were removed from the analysis and subjected to further investigation. Analysing the outliers, it was possible to observe that the samples that correspond to lines 13, 15, 16 and 29, characterised by the positive curvature of 0.1 and large overhang length, underwent warping problems, as it was possible to observe in Figure 7(a), in which the nominal geometry was compared with the measured one. For these samples, the area near the

edges excluded in the analysis was not sufficient to remove the edge effect. The sample which corresponds to line 36, instead, was characterised by a very high value of minimum deviation (8.57 mm) and it was possible to ascribe this to a software bug during the comparison of the nominal surface and the points cloud. Error in this last sample was thus corrected and data was used to verify the results of the analysis.

Figure 5 Distribution of the surface quality index *k* values calculated for the analysed specimens (see online version for colours)

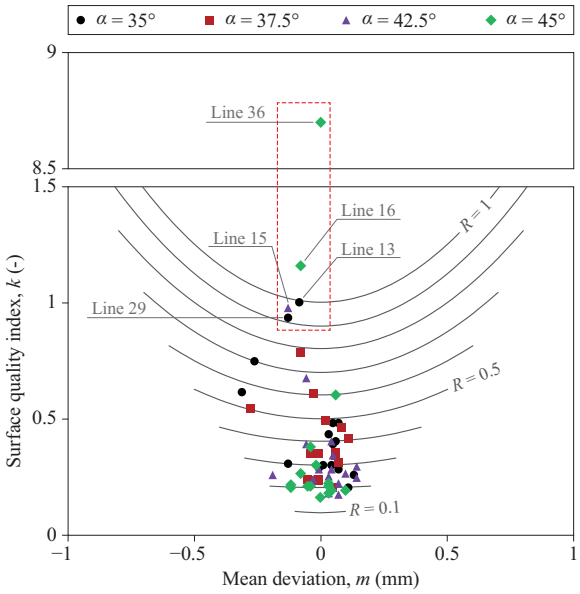

Note: The outliers are in the red dashed box.

Figure 6 Boxplot of the surface quality index *k* values calculated for the analysed specimens (see online version for colours)

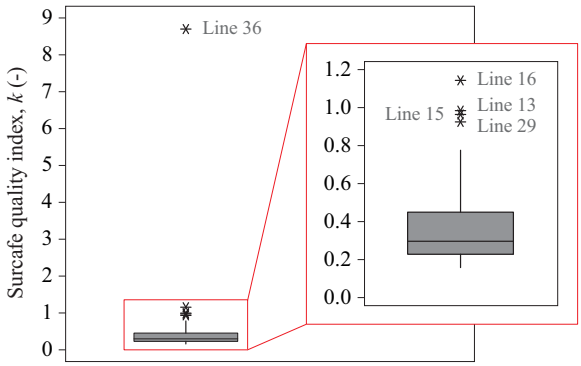

Figure 7 Examples of surfaces characterised by (a) negative and (b) positive mean deviation for specimens that correspond to lines 29 and 63, respectively (see online version for colours)

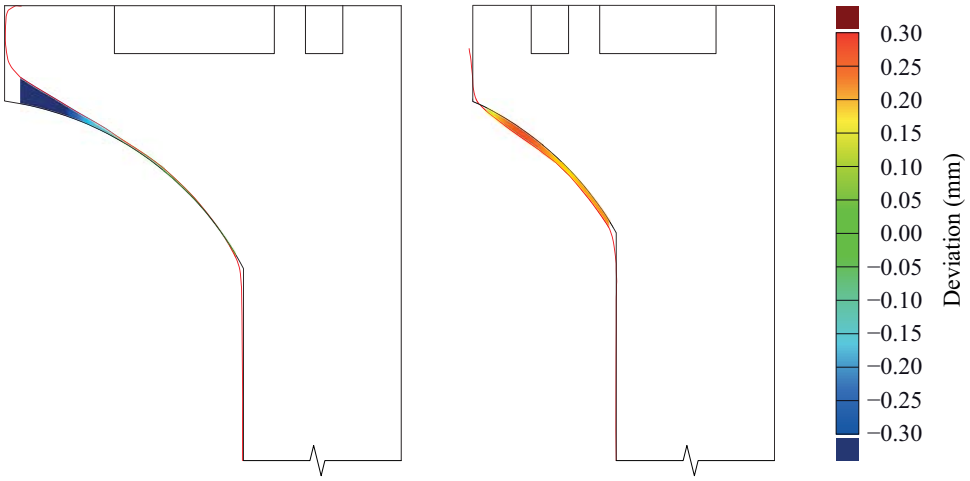

(a) (b)

Table 5 Results of the analysis of variance

Source	*DF*	*Adj SS*	*Adj MS*	*F-value*	*P-value*	
Model	36	1.49204	0.04145	8.60	0.0000	
Linear	9	0.85438	0.09493	19.69	0.0000	
Δx	3	0.28047	0.09349	19.39	0.0000	Highly significant
$1/R$	3	0.44873	0.14958	31.03	0.0000	Highly significant
α	3	0.25791	0.08597	17.83	0.0000	Highly significant
2-way interactions	27	0.52498	0.01944	4.03	0.0010	
$\Delta x \cdot 1/R$	9	0.40733	0.04526	9.39	0.0000	Highly significant
$\Delta x \cdot \alpha$	9	0.07507	0.00834	1.73	0.1410	
$1/R \cdot \alpha$	9	0.08283	0.00920	1.91	0.1040	
Error	22	0.10606	0.00482			
Total	58	1.59810				

Note: S = 0.069432, R^2 = 93.36%, R^2adj = 82.50%.

After eliminating the outliers, highlighted in italic font in Table 4, the ANOVA (Table 5) indicates that the DoE was able to explain about 82% of the variation of the selected response. The factors that were significant for the analysis were point out. It was possible to observe that all the geometrical factors (Δx, $1/R$ and α) significantly influenced the value of surface quality index k. Moreover, considering the interactions between the selected factors, the interaction between Δx and $1/R$ had a great influence on the value of the response. The interactions between Δx and α, and $1/R$ and α were not statistically significant from this analysis.

Figure 8 Main effect plot for the surface quality index k (see online version for colours)

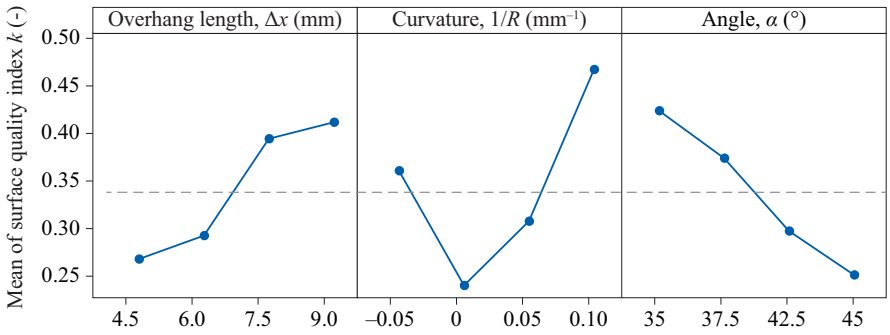

Figure 9 Interaction plot for the surface quality index k (see online version for colours)

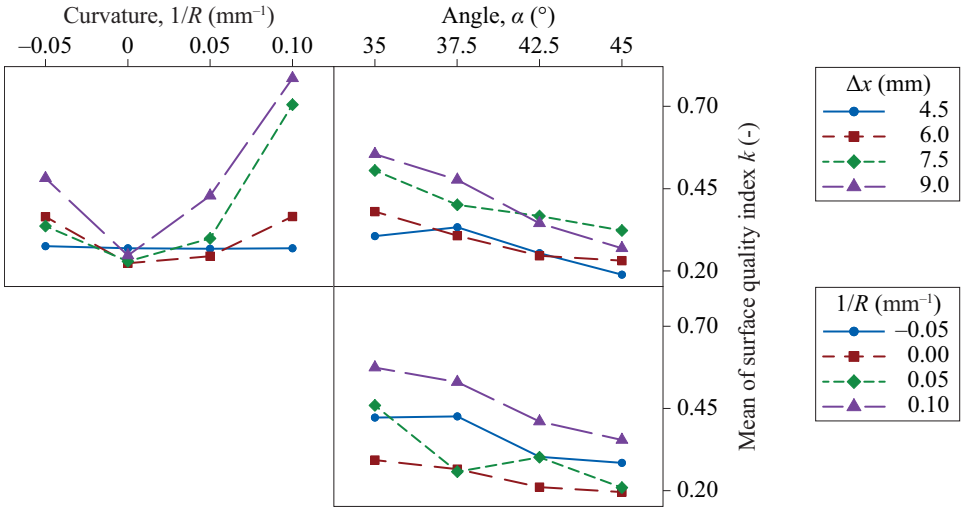

Main effect plot, reported in Figure 8, gives a visual illustration of the results reported in Table 5. In particular, the slope of the line between two different levels depicts the power of influence of the examined factor. It can be observed that surface quality index k increases as the overhang length increases, with a sharp variation when the factor Δx varies from 6 mm to 7.5 mm. The most critical level for the factor Δx was 9 mm, which corresponds to the overhang with the greater extension. From Table 4 and Figure 5, it is evident that the highest observed values of the surface quality index k are associated to negative mean values. Looking at the cases with large overhangs, it is observed that the value of the mean m, in most cases, was negative and this behaviour was probably related to the warping defect caused by thermal stresses induced by the process. Actually, a negative m value means that less material than nominal is detected. On the contrary, if the mean deviation m is positive, it means that a major quantity of material respect to the nominal was present (Figure 7). In general, this was expected, because more material is a consequence of the slicing operations and stairstepping phenomenon. Moreover, other effects can occur on the part surface, such as a growing effect, related to the incorporation of partially sintered particles, surface irregularities due to gravity effects on

melt pool and capillarity. Considering the factor $1/R$, it was possible to note that a small curvature, both positive or negative, has a little influence on the value of the surface quality index k, whereas if the curvature becomes larger ($1/R$ = 0.1 mm^{-1}) an abrupt variation was observed. Again, it is observed from Table 4 that the mean m becomes negative. In fact, by increasing the curvature, the slope of the tangent line to the surface decreases as approaching the edge, as it tends to zero and warping occurs. The effect of the angle α on the quality of overhanging surfaces is confirmed and the surface quality index k decreases the tilting angle α increases. From the analysis it was possible to observe that none of the samples has a surface quality index k largely greater than zero, the major value, in fact, is 0.67, excluding outliers. If the value of the surface quality index k is almost zero it means that the resulting geometry has a little deviation respect to the nominal one, so the mean deviation m and range r are both small. The surface quality index k value almost nil was associated to the samples with a radius of curvature infinite, so with planar surfaces, and with a small overhang length.

Figure 10 Graphical representation of the surface quality index k statistical regression model as a function of curvature, overhang length and α angle, (a) α = 35° (b) α = 37.5° (c) α = 42.5° (d) α = 45° (see online version for colours)

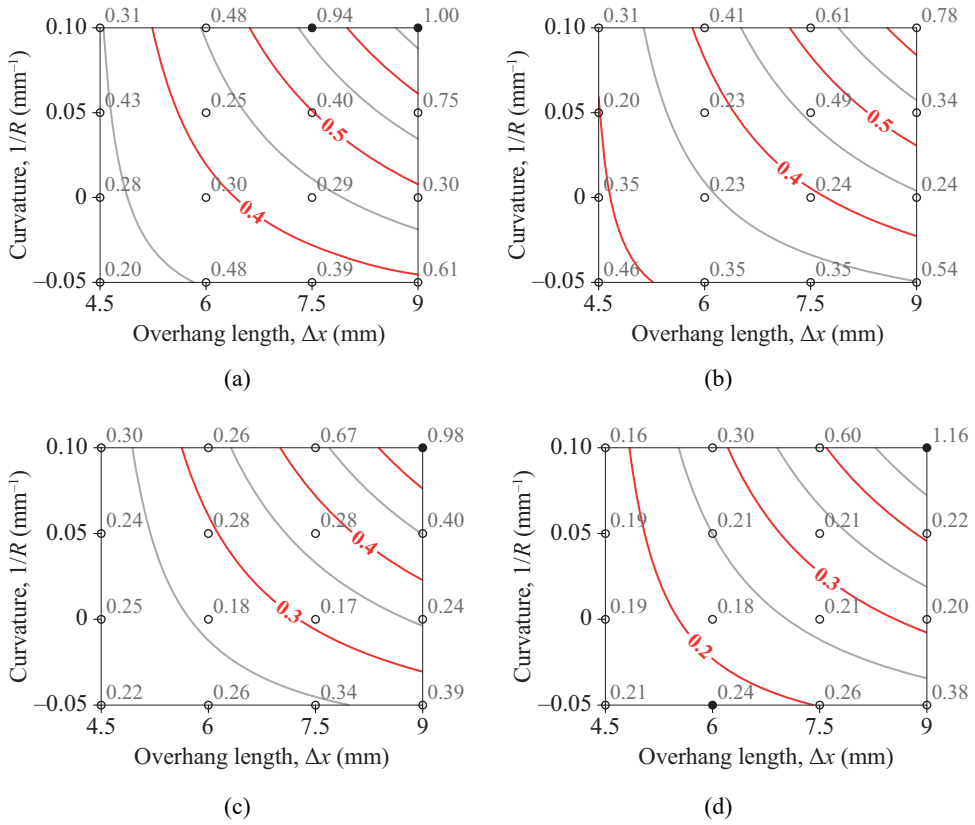

Note: Black points correspond to the lines 13, 15, 16, 29 and 36.

From the interaction plot in Figure 9 it was possible to observe the strong interaction between the factors Δx and $1/R$. In particular, the effect of overhang length Δx is more powerful if the value of curvature increases. Whereas, a small value of angle α slightly increases the sensitivity of the surface quality index k to the curvature $1/R$. As detailed above, both the increase in the curvature and the decrease in the angle α highly influence the variation of the surface slope, raising the risk of warpage and dross formation. The interaction between Δx and α does not significantly influence the value of the surface quality index k.

Then, a regression analysis was performed in order to estimate a mathematical relation between the factors, their interactions and the examined response. The data sets yielded the following equation

$$k = 0.641 + 0.040 \cdot \Delta x - 4.020 \cdot 1/R - 0.014 \cdot \alpha + 0.820 \cdot \Delta x \cdot 1/R \quad (2)$$

The regression equation (2) gives an R^2_{adj} = 51%. The result is plotted in Figure 10 in which the black dots correspond to the lines 13, 15, 16, 29 and to the line 36, after correction. From graphs in Figure 10 it is possible to observe in which way the combination of overhang length and curvature influences the value of the surface quality index k. Each graph was plotted considering the factor α as a constant and each curve corresponds to a specific value of the surface quality index k. In general, the quality of the surface decreases (k value gets higher, with a maximum of 1.16 for the analysed samples) if both overhang length and curvature are high. As a matter of fact, the detected outliers are located in the upper right end of all the four diagrams. From Figure 10, it is evident that typically a high value of the surface quality index k is obtained for high values of overhang length and curvature, and small inclination angle. In these conditions, the mean deviation is usually negative and the range is high as warping occurs. As expected, best values of the surface quality index k are found for small overhang length and curvature, and large inclination angle. For angle α lower than 37.5°, the analysis shows that, in general, the combination of small overhang length and low curvature leads to low positive deviation and small range, and the surface quality is good. The positive mean deviation is an indicator that more material than the nominal geometry is present, since surface irregularities are generated during process, such as for instance stair-stepping or surface growing. However, these defects did not significantly alter the surface geometry. For angle α greater than 42.5°, the surface quality was typically good and the surface quality index k value ranged from 0.2 and 0.3, with the only exception of samples obtained with both high overhang length and high curvature, as evidenced before.

6 Conclusions

In this study, a specific index has been defined, in order to evaluate the quality of overhang surfaces. The surface quality index k combines information about the mean deviation of the actual surface from the nominal one and the range of the variation. From the experimental analysis it is possible to point out that the overhang length (Δx), the angle α and the curvature ($1/R$) strongly influence the quality of an overhanging surface. In addition, also the interaction between Δx and $1/R$ and α has a strong impact on the surface quality.

The surface quality index k is adequate to describe the quality of the surface for different combinations of parameters. Especially, it is found that the surface quality increases as the surface quality index k tends to zero, with a good quality for k score less than 0.3. Through the analysis of the experimental results, it is possible to correlate high values of the surface quality index k to some possible problems that occur during the L-PBF process. In particular, high values of the surface quality index k are typically associated with negative values of mean m and large range of variation r. This behaviour is ascribed to a warping defect and the analysed surface is characterised by a lack of material. On the contrary, a positive mean deviation is the consequence of a greater quantity of material respect to the nominal geometry and some possible causes are the aggregation of sintered particles, surface irregularities due to gravity effect and capillarity, and the stairstepping phenomenon. However, these defects significantly affect the surface quality only for inclination angle lower than 37.5º and large overhang extensions, leading to surface quality index k values up to 0.5.

The outcomes of this analysis could be used to develop preliminary design rules in order to produce overhangs by minimising the use of support structures and controlling the surface quality. In detail:

- a surface quality index value less than 0.4 is an indication of good surface quality
- the surface quality is better for small overhang length and curvature, and large inclination angle
- for angle α lower than 37.5º, in case of AlSi10Mg, the combination of overhang length less than 6 mm and low curvature leads to low positive deviation and small range of deviation, and the surface quality is good.

Acknowledgements

The authors would like to acknowledge Mr. Giovanni Marchiandi and Dr. Andrea Scavino for their help and support in the measurement campaigns.

References

Atzeni, E. and Salmi, A. (2012) 'Economics of additive manufacturing for end-usable metal parts', *The International Journal of Advanced Manufacturing Technology*, Vol. 62, Nos. 9–12, pp.1147–1155.

Atzeni, E. and Salmi, A. (2015) 'Study on unsupported overhangs of AlSi10Mg parts processed by direct metal laser sintering (DMLS)', *Journal of Manufacturing Processes*, Vol. 20, No. 3, pp.500–506.

Atzeni, E., Iuliano, L., Minetola, P. and Salmi, A. (2010a) 'Redesign and cost estimation of rapid manufactured plastic parts', *Rapid Prototyping Journal*, Vol. 16, No. 5, pp.308–317.

Atzeni, E., Iuliano, L., Minetola, P., Salmi, A. and Gatto, A. (2010b) 'Artificial teeth manufacturing: inspection of mould and teeth by contactless scanning systems', in Bartolo, P. et al. (Eds.): *Innovative Developments in Design and Manufacturing – Advanced Research in Virtual and Rapid Prototyping*, CRC Press, Leiria, Portugal, pp.131–136.

Atzeni, E., Minetola, P. and Salmi, A. (2013) 'Dimensional analysis of a prototype mould-making process for thermoplastic resin transfer moulding', *The International Journal of Advanced Manufacturing Technology*, Vol. 65, Nos. 1–4, pp.309–317.

Baudana, G., Biamino, S., Klöden, B., Kirchner, A., Weißgärber, T., Kieback, B., Pavese, M., Ugues, D., Fino, P. and Badini, C. (2016) 'Electron beam melting of Ti-48Al-2Nb-0.7Cr-0.3Si: feasibility investigation', *Intermetallics*, Vol. 73, pp.43–49.

Brackett, D., Ashcroft, I. and Hague, R. (2011) 'Topology optimization for additive manufacturing', *Proceedings of the Solid Freeform Fabrication Symposium*, Austin, TX, pp.348–362.

Calignano, F. (2014) 'Design optimization of supports for overhanging structures in aluminum and titanium alloys by selective laser melting', *Materials & Design*, Vol. 64, pp.203–213.

Calignano, F., Manfredi, D., Ambrosio, E., Iuliano, L. and Fino, P. (2013) 'Influence of process parameters on surface roughness of aluminum parts produced by DMLS', *International Journal of Advanced Manufacturing Technology*, Vol. 67, Nos. 9–12, pp.2743–2751.

Fox, J.C., Moylan, S.P. and Lane, B.M. (2016) 'Effect of process parameters on the surface roughness of overhanging structures in laser powder bed fusion additive manufacturing', *Procedia CIRP*, Vol. 45, pp.131–134.

Gan, M. and Wong, C. (2016) 'Practical support structures for selective laser melting', *Journal of Materials Processing Technology*, Vol. 238, pp.474–484.

Gao, W., Zhang, Y., Ramanujan, D., Ramani, K., Chen, Y., Williams, C.B., Wang, C.C., Shin, Y.C., Zhang, S. and Zavattieri, P.D. (2015) 'The status, challenges, and future of additive manufacturing in engineering', *Computer-Aided Design*, Vol. 69, pp.65–89.

Gu, D. (2015) *Laser Additive Manufacturing of High-Performance Materials*, Springer, Berlin, Heidelberg.

Gu, D., Meiners, W., Wissenbach, K. and Poprawe, R. (2012) 'Laser additive manufacturing of metallic components: materials, processes and mechanisms', *International Materials Reviews*, Vol. 57, No. 3, pp.133–164.

Herzog, D., Seyda, V., Wycisk, E. and Emmelmann, C. (2016) 'Additive manufacturing of metals', *Acta Materialia*, Vol. 117, pp.371–392.

ISO/ASTM52900-15 (2015) *Standard Terminology for Additive Manufacturing – General Principles – Terminology*, ASTM International, West Conshohocken, PA.

Iuliano, L. and Minetola, P. (2009) 'Enhancing moulds manufacturing by means of reverse engineering', *The International Journal of Advanced Manufacturing Technology*, Vol. 43, No. 5, pp.551–562.

Iuliano, L., Minetola, P. and Salmi, A. (2010) 'Proposal of an innovative benchmark for comparison of the performance of contactless digitizers', *Measurement Science and Technology*, Vol. 21, No. 10, pp.105102–105114.

Jardini, A.L., Larosa, M.A., Filho, R.M., Zavaglia, C.A.d.C., Bernardes, L.F., Lambert, C.S., Calderoni, D.R. and Kharmandayan, P. (2014) 'Cranial reconstruction: 3D biomodel and custom-built implant created using additive manufacturing', *Journal of Cranio-Maxillofacial Surgery*, Vol. 42, No. 8, pp.1877–1884.

Liu, R., Wang, Z., Sparks, T., Liou, F. and Newkirk, J. (2017) 'Aerospace applications of laser additive manufacturing', in *Laser Additive Manufacturing*, Elsevier, Amsterdam, Netherlands.

Manfredi, D., Calignano, F., Krishnan, M., Canali, R., Ambrosio, E.P. and Atzeni, E. (2013) 'From powders to dense metal parts: characterization of a commercial AlSiMg alloy processed through direct metal laser sintering', *Materials*, Vol. 6, No. 3, pp.856–869.

Minetola, P. (2012) 'The importance of a correct alignment in contactless inspection of additive manufactured parts', *International Journal of Precision Engineering and Manufacturing*, Vol. 13, No. 2, pp.211–218.

Minetola, P., Iuliano, L. and Argentieri, G. (2012) 'Contactless inspection of castings: analysis of alignment procedures', *International Journal of Cast Metals Research*, Vol. 25, No. 1, pp.38–46.

Minetola, P., Iuliano, L. and Calignano, F. (2015) 'A customer oriented methodology for reverse engineering software selection in the computer aided inspection scenario', *Computers in Industry*, Vol. 67, pp.54–71.

Salmi, A., Atzeni, E., Calignano, F., Minetola, P. and Iuliano, L. (2014) 'Combined reverse engineering and CAD approach for mould modelling in casting simulation', *International Journal of Cast Metals Research*, Vol. 27, No. 4, pp.213–220.

Shellabear, M. and Nyrhilä, O. (2004) 'DMLS-Development history and state of the art', *Laser Assisted Netshape Engineering 4*, *Proceedings of the 4th LANE*, pp.21–24.

Strano, G., Hao, L., Everson, R.M. and Evans, K.E. (2013) 'Surface roughness analysis, modelling and prediction in selective laser melting', *Journal of Materials Processing Technology*, Vol. 213, No. 4, pp.589–597.

Tanco, M., Viles, E., Ilzarbe, L. and Álvarez, M.J. (2007) 'Manufacturing industries need design of experiments (DoE)', *World Congress on Engineering*, pp.1108–1112.

Thomas, D. (2009) *The Development of Design Rules for Selective Laser Melting*, University of Wales.

Vora, P., Mumtaz, K., Todd, I. and Hopkinson, N. (2015) 'AlSi12 in-situ alloy formation and residual stress reduction using anchorless selective laser melting', *Additive Manufacturing*, Vol. 7, pp.12–19.

Wang, D., Yang, Y., Liu, R., Xiao, D. and Sun, J. (2013a) 'Study on the designing rules and processability of porous structure based on selective laser melting (SLM)', *Journal of Materials Processing Technology*, Vol. 213, No. 10, pp.1734–1742.

Wang, D., Yang, Y., Yi, Z. and Su, X. (2013b) 'Research on the fabricating quality optimization of the overhanging surface in SLM process', *The International Journal of Advanced Manufacturing Technology*, Vol. 65, Nos. 9–12, pp.1471–1484.

Xie, L., Wen, Y., Wang, L., Jiang, C. and Ji, V. (2016) 'Characterization on surface properties of Ti-6Al-4V after multiple shot peening treatments', *Journal of Engineering Materials and Technology*, Vol. 138, No. 4, p.041005.